

Charge trapping in optimally doped epitaxial manganite thin filmsM. Bibes,^{1,2,*} S. Valencia,¹ Ll. Balcells,¹ B. Martínez,¹ J. Fontcuberta,¹ M. Wojcik,³ S. Nadolski,³ and E. Jedryka³¹*Institut de Ciència de Materials de Barcelona, CSIC, Campus de la UAB, E-08193 Bellaterra, Catalunya, Spain*²*Unité Mixte de Physique THALES/CNRS, Domaine de Corbeville, 91404 Orsay, France*³*Institute of Physics, Polish Academy of Sciences, Al. Lotników 32/46, 02-668 Warszawa, Poland*

(Received 18 April 2002; revised manuscript received 15 July 2002; published 21 October 2002)

We have studied the thickness dependence of the magnetotransport properties of $\text{La}_{2/3}\text{Ca}_{1/3}\text{MnO}_3$ thin films epitaxially grown on SrTiO_3 , LaAlO_3 , and NdGaO_3 single-crystalline substrates. When thickness decreases, a global disruption of the magnetoelectronic properties occurs, namely the resistivity and the low-temperature magnetoresistance increase while the metal-to-insulator transition temperature (T_P) is lowered. We state that the electronic properties of these films, especially close to the film/substrate interface, differ from those of the bulk material. This is confirmed by nuclear-magnetic-resonance measurements which provide evidence that these films have an inhomogeneous magnetoelectronic nanostructure with distinguishable regions containing localized charges. These regions are scattered within the films, with a higher density close to interfaces in the case of $\text{La}_{2/3}\text{Ca}_{1/3}\text{MnO}_3$ films on SrTiO_3 but more homogeneously distributed for films grown on NdGaO_3 . Since our manganite films have a virtually unrelaxed crystal structure, the thickness dependence of T_P can neither be related to the strain states nor to dimensional effects. Alternatively, we show that the coexistence of different electronic phases leads to a modification of the carrier density in the metallic regions and, presumably, to an enhancement of the disorder in the Mn-O bond length and Mn-O-Mn angles. We will argue that the conjunction of both factors promotes a decrease of the double exchange transfer integral and, consequently, accounts for the reduction of the Curie temperature for the thinnest films. The possible mechanisms responsible for this phase separation are discussed in terms of the microstructure of the interfaces between the manganite and the insulating perovskite.

DOI: 10.1103/PhysRevB.66.134416

PACS number(s): 75.30.Vn, 75.70.Ak, 76.60.Lz

I. INTRODUCTION

Perovskites based on transition-metal oxides show a large number of properties related to the many competing interactions between charge, spin and lattice.^{1,2} This versatility allows the design of heterostructures based on oxide compounds with very promising properties. Among these, the best known are probably tunnel junctions based on half metallic manganites such as $\text{La}_{2/3}\text{Sr}_{1/3}\text{MnO}_3$ (Refs. 3 and 4) (LSMO) and $\text{La}_{2/3}\text{Ca}_{1/3}\text{MnO}_3$ (Ref. 5) (LCMO), but spin-valves structures⁶ or spin injectors⁷ have also been fabricated. However, the response of such devices is generally limited, like in the case of tunnel junctions for which the magnetoresistance becomes vanishingly small well below the Curie point of the electrodes. Several studies suggest that this is probably due to a loss of spin polarization at interfaces.^{8,9} It is therefore of great importance to determine the properties of these interfaces in order to better understand the reasons for depolarization and enhance the response of these promising devices.

There are different methods for studying the properties of manganite-insulator interfaces. Among them, neutron reflectometry¹⁰ and electron energy-loss spectroscopy¹¹ can probe the magnetic and/or electronic properties locally. Another approach is to characterize the interfaces by analyzing the thickness dependence of the magnetoelectronic properties of films grown on different substrates. In this case, it would be desirable that the films have similar microstructure, irrespective of their thickness, so that the effect of defects such as dislocations and twin boundaries can be avoided and the study reveals indeed the properties of the interface. This

is difficult to achieve in practice and the structure of the films usually relaxes for thickness values above some critical value.¹²⁻¹⁴ However, we have shown in a previous study that under appropriate conditions it is possible to fabricate a series of films of $\text{La}_{2/3}\text{Ca}_{1/3}\text{MnO}_3$ (LCMO) on SrTiO_3 (STO) of thicknesses ranging from a few nm to more than 100 nm with virtually constant in-plane (a) and out-of-plane parameters (c).¹⁵

When the properties of epitaxial films of manganite are studied as a function of thickness (t), two major features are usually observed. First, the resistivity increases when t is reduced, which has been interpreted as due to the presence of an insulating dead layer located at interfaces.^{16,17} This is often accompanied by a decrease of the magnetic moment and magnetically dead layers have also been detected recently.^{14,18} The thickness of these dead layers is on the order of a few nm and varies with the nature of the substrate. It has also been found that when t is lower than a critical value, LSMO and LCMO films are insulating in the whole temperature range.¹⁹⁻²¹ Second, several publications have reported a reduction of the Curie point T_C and of the metal-to-insulator transition temperature T_P of LSMO and LCMO films with respect to bulk values when t decreases. This can be the case for films with a gradually relaxed structure¹²⁻¹⁴ but also in fully strained films.²² This last observation is a conclusive indication that strain cannot be the only factor responsible for the reduction of T_C in very thin films.

Rather little theoretical work has been done on strain issues for manganite films. Millis and co-workers have analyzed the problem and state that one must distinguish between uniform bulk strain ϵ_B and biaxial strain ϵ^* effects²³

on the Curie point. Namely, ϵ_B can lead to an increase or a decrease of T_C depending on the sign of the strain, while biaxial strain favors electron localization in e_g levels split by static Jahn-Teller distortion, causing T_C to decrease. Rao *et al.* have tried to explain results obtained for LCMO films on STO and LaAlO₃ (LAO) with this model and found that it did not account for the observed decrease of T_C upon thickness reduction.¹³ Alternatively, a recent study showed that a biaxial tensile strain can lead to an enhancement of T_C in La_{1-x}Ba_xMnO₃ films due to orbital degeneracy effects.²⁴ Nevertheless, this is not expected to cause an increase of T_C in the La_{1-x}Ca_xMnO₃ system.²⁵

In a previous work on LCMO/STO interfaces, we have found evidence of multiple phase separation into ferromagnetic-metallic, ferromagnetic-insulating, and nonferromagnetic-insulating regions. The nucleation of non-metallic regions appears to be related to a modification of the carrier density in the metallic phase which causes the Curie temperature to decrease for thinner films.²⁶ This change in the effective doping value induced by phase separation can be considered as a third possible factor responsible for the thickness dependence of T_C in manganite films, in addition to stress and orbital degeneracy effects.

In order to obtain more information about the effect of these different factors on fundamental issues such as the thickness dependence of the Curie temperature or the origin and characterization of dead layers, we have performed a systematic study of the thickness dependence ($2.4 < t < 108$ nm) of the magnetotransport properties of LCMO films deposited on three different substrates: SrTiO₃, LaAlO₃ (LAO), and NdGaO₃ (NGO). Apart from the thicker films ($t > 54$ nm) on LAO that show partial structural relaxation, the LCMO grows almost fully strained on the substrates. This requirement is thought to provide almost ideally sharp interfaces and a low density of microstructural defects (such as dislocations), thus allowing the characterization of the interface with the substrate through the thickness dependence of the magnetoelectronic properties. For these three substrates, the mismatch values are +1.17% (STO), -1.81% (LAO), and -0.08% (NGO) which leads to a tensile, compressive, and almost negligible strain state, respectively. In addition, we should mention that STO and LAO are cubic materials at the deposition temperature while NGO is orthorhombic. The results section of this paper is divided in five parts dedicated to structural analysis, temperature dependence of the resistivity, thickness dependence of T_p , magnetoresistance measurements, and finally the results of nuclear-magnetic-resonance experiments. All these data point towards a nonhomogeneous magnetoelectronic texture of the manganite with electron trapping in nonmetallic regions, which is proven to be closely linked to the thickness dependence of T_p . This correlation and the origin of the phase separation are discussed in the last section.

II. EXPERIMENT

The films used in this study were grown by rf sputtering at a temperature of 775 °C and a pressure of 225 mtorr. More details on the growth procedure can be found in Ref. 27. We

used single-crystalline commercial substrates (Crystec, GmbH) of STO ($a = 3.905$ Å), LAO ($a = 3.79$ Å), and both (001)-oriented (cubic notation) and (110)-oriented NGO (orthorhombic notation). In the latter case, there are two slightly nonequivalent distances in the plane ($a = 3.853$ Å and $a' = 3.861$ Å cubic notation). Besides, while LAO is cubic at the deposition temperature, it becomes rhombohedral upon cooling with a phase transition at 544 °C.²⁸ This symmetry breaking can give rise to orientation variants in the low-temperature phase of LAO and, consequently, in the LCMO film. The root-mean-square surface roughness of the as-received substrates was measured by atomic force microscopy and estimated to be 0.15–0.2 nm.

The x-ray-diffraction analysis was performed on a Philips MRD system allowing for the detection of symmetric and asymmetric reflections. The thickness of the films was checked by x-ray reflectometry. The magnetotransport properties were measured in a four-probe configuration with a Quantum Design physical properties measurement system (PPMS) in the temperature range 10–350 K and with a maximum field of 90 kOe applied perpendicular to the plane of the samples. Gold pads were deposited on the films and contacts were made by attaching platinum wires to the samples with silver paste. A Quantum Design superconducting quantum interference device (SQUID) was used to measure the magnetic properties with the field applied in plane. NMR spectra have been measured at 4.2 K by using a broadband phase-sensitive spin-echo spectrometer. For each sample, several NMR spectra were recorded by measuring spin-echo amplitude in the frequency range 300–450 MHz with steps of 1 MHz, at zero external magnetic field and a constant excitation rf field h_1 which was varied by more than an order of magnitude. More than $N \approx 10^6$ data were acquired at each frequency in order to improve the signal-to-noise ratio. At each frequency point the intrinsic NMR enhancement factor and the restoring field acting on the electronic magnetization have been determined from the h_1 dependence of signal intensity. The final NMR spectrum for each sample has been determined taking into account the intrinsic enhancement factor and usual ω^2 correction of signal intensity. The details of the NMR procedure will be described elsewhere.²⁹

III. RESULTS

A. Structure

In Fig. 1, we show $\Theta - 2\Theta$ scans close to the (002) reflections for several LCMO films grown on STO. The angular position of these reflections and the associated values of the out-of-plane parameters c of the films are listed in Table I, together with those of the a parameters, as deduced from the position of the (103) reflections. Since the cell parameter for bulk LCMO is 3.86 Å, the obtained values for c indicate that the LCMO is under tensile strain. Even though the position of the (002) reflection is closely coincident for all the films, irrespective of thickness, a small shift can be detected, signaling a residual, weak structural relaxation. For all these films, a is very close to the cell parameter of STO which confirms that the LCMO is heavily strained.

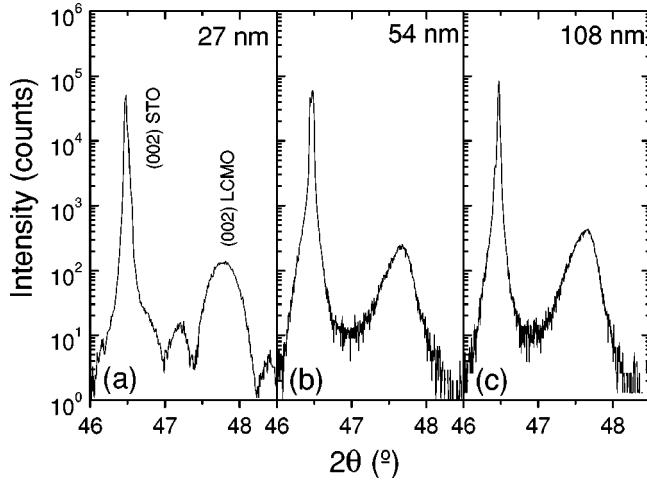


FIG. 1. High-resolution $\Theta-2\Theta$ scans close to the (002) reflections of the LCMO and of the STO for films of three different thickness values.

In addition, clear Laue fringes can be seen adjacent to the (002) peak of the LCMO for the 27-nm film. Their spacing closely corresponds to the thickness of the film deduced from x-ray reflectometry measurements. This indicates that this film consists of coherently strained material. Laue fringes are absent from the scans of the 54- and 108-nm films which can be a natural consequence of the decrease of the intensity of the high order peaks for larger thickness values. However, we cannot exclude that it may be due to a slight structural relaxation, possibly accompanied by a narrow distribution of cell parameters.

In the case of films on LAO, a different situation takes place as illustrated by Fig. 2. For films up to thicknesses of 54 nm, c is roughly constant and its value indicates a heavily strained (compressive) material. Laue fringes are not observed. For a 108-nm film, two peaks can be assigned to the (004) reflection of the LCMO, presumably corresponding to two regions with different strain states. Films on NGO were also characterized by x-ray diffraction but since the cell parameters of LCMO and NGO are virtually identical, no quantitative analysis of the strain states could be made. However, it is reasonable to expect that all the LCMO films grown on NGO are fully epitaxial and have the same crystallographic structure.

B. Resistivity vs temperature

In Fig. 3 we plot the temperature dependence of the resistivity in zero field for films of various thicknesses grown on

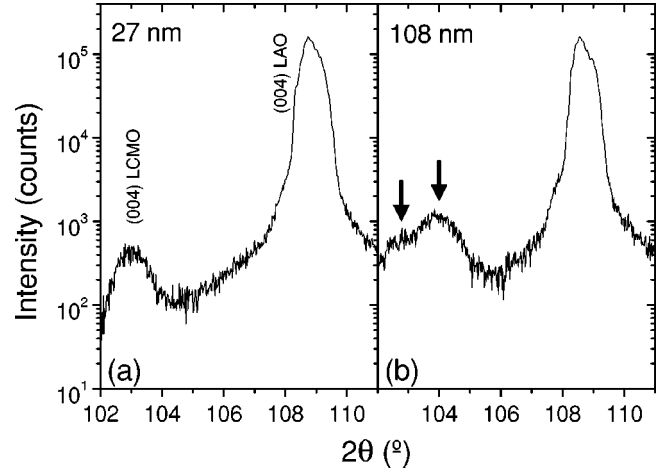


FIG. 2. $\Theta-2\Theta$ scans close to the (004) reflections of the LCMO and of the LAO for two films of different thickness. Arrows indicate the position of the peaks assigned to the (004) reflection of LCMO.

STO [Fig. 3(a)], LAO [Fig. 3(b)], and NGO [Fig. 3(c)]. Thicker films show a bulklike behavior with a crossover between a low-temperature metallic dependence and a high-temperature thermally activated transport at $T_p \approx 263$ K for films on LAO and NGO. The 108-nm film grown on STO has a Curie temperature of about 260 K, as deduced from SQUID measurements. The residual resistivity at 10 K is in the 200–300- $\mu\Omega$ -cm range for the films grown on NGO with $t > 100$ nm while it is some 600 $\mu\Omega$ cm for the 108-nm-thick film on LAO. This is close to the values reported in the literature.

When t decreases the resistivity increases gradually in the whole temperature range and T_p shifts to values as low as 110–130 K for the 6- and 12-nm-thick films on STO and the 6-nm film on NGO. This is particularly striking since, as deduced from the structural analysis, the cell parameters of the manganite are virtually identical within the same series of films for a given substrate. Furthermore, 108-nm films on NGO, STO, and LAO show transitions at very similar temperatures irrespectively of their strain states. Another remarkable feature is that the resistivity of the films shows an insulating dependence in the whole accessible temperature range when t is lower than a critical thickness $t_{ins} = 6$ nm for LCMO/STO and LCMO/NGO samples and $t_{ins} = 12$ nm for LCMO/LAO. For these insulating films, no metallic behavior could be induced even when applying a field of 90 kOe. The

TABLE I. Results from the x-ray diffraction analysis for some of the LCMO films.

Substrate	t (nm)	2θ (°)	c (Å)	$\Delta c/c_{bulk}$ (%)	a (Å)	$\Delta a/a_{bulk}$ (%)	ϵ_B	ϵ^*
STO	27	47.78(2) ^a	3.804	1.451	3.903	-1.114	-0.259	1.283
STO	54	47.66(5) ^a	3.812	1.244	3.902	-1.088	-0.310	1.166
STO	108	47.64(8) ^a	3.814	1.192	3.894	-0.881	-0.190	1.037
LAO	27	102.98 ^b	3.941	-2.098	3.799	1.580	0.354	-1.839
LAO	108	102.76 104.03 ^b	3.947, 3.912	-2.253, -1.347	3.820	1.036	-0.060, 0.242	-1.644, -1.191

^a(002) reflection.

^b(004) reflection.

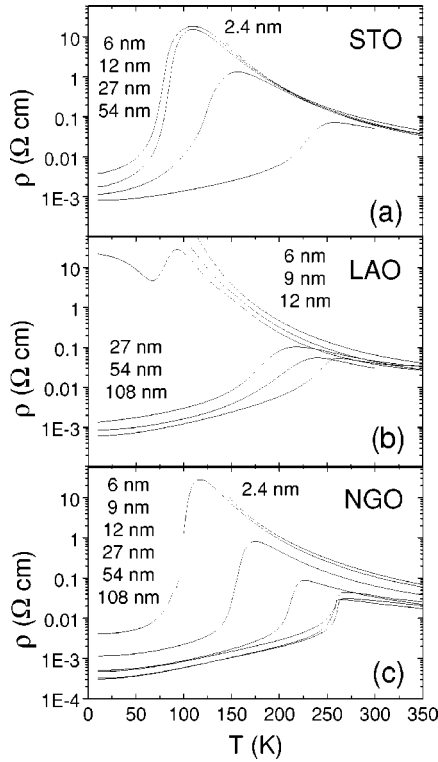


FIG. 3. Temperature dependence of the resistivity for the three series of LCMO films.

12-nm film on LAO shows a metal-to-insulator transition around 95 K but becomes insulating for $T < 65$ K.

From this rough analysis, it appears that the properties of the LCMO films are strongly altered by the reduction of thickness, i.e., by the proximity of the interface with any of the three substrates used. Nonmetallic regions are present in agreement with previous results of the literature. The modification of the electric properties at interfaces can be better monitored by plotting the conductance G of the films in function of thickness; see Fig. 4. If we fit the data with a linear dependence, a good agreement is obtained in the case of NGO and STO. Assuming a linear extrapolation of G for small thickness values, we find that G becomes zero at a finite thickness which can be interpreted as reflecting the presence of nonconducting material close to the substrate. In the case of LAO, the linear fit is not as good. Although there is no reason *a priori* to presume that a linear extrapolation should work, the fact that this simple model holds for STO and NGO but not for LAO suggests that this may be due to structural relaxation which occurs at $t \geq 54$ nm in the LCMO/LAO series.

The thickness of this extrapolated dead layer t_{dead} depends on the substrate and is 6.7 ± 2 nm for STO, 15.3 ± 4 nm for LAO, and 6.7 ± 2 nm for NGO. The stronger disruption of the transport properties in the case of LAO is confirmed by these plots. However, if these values give the approximate amount of material which is not metallic, a model of a conduction in parallel between a metallic layer of thickness $t - t_{\text{dead}}$ and a dead layer is far too simple to explain the thickness dependence of the global magnetotransport properties, such as, for instance, the gradual decrease of T_P . This ob-

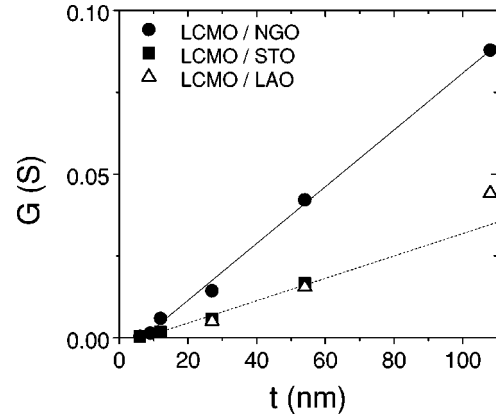


FIG. 4. Thickness dependence of the conductance of the LCMO films measured at 10 K. The solid and dashed lines correspond to linear fits to the data for LCMO/NGO and LCMO/STO, respectively.

servation is a first indication that the increase in resistivity is probably more gradual and, consequently, that regions with high resistivity could be present at distances from the interface larger than t_{dead} .

C. Thickness dependence of T_P

Now we come back to the thickness dependence of T_P , which is plotted in Fig. 5, along with that of T_C as deduced from magnetization curves measured with a field of 1 kOe (not shown). These two temperatures coincide closely which confirms that transport properties present a negligible contribution from structural defects. A systematic decrease of T_P is observed for the three series. However, the shape of the T_P vs t curves depends on the substrate. For films on STO, a rapid decrease is observed for $20 < t < 50$ nm, and T_P stabilizes around 120 K for the 6- and 12-nm films. In the case of

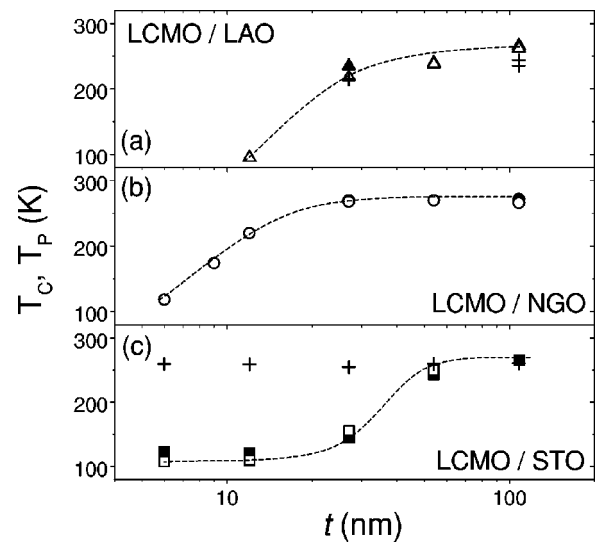


FIG. 5. Thickness dependence of the Curie point (solid symbols) and of the metal-to-insulator transition temperature (open symbols) for the LCMO films. Crosses represent values obtained for the model of Eq. 1.

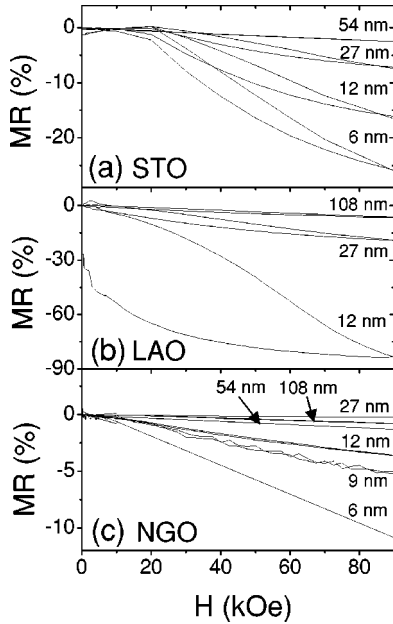


FIG. 6. Field dependence of the magnetoresistance of films of different thicknesses on STO (a), LAO (b), and NGO (c) at 10 K.

LAO, the rapid decrease takes place for $t < 25$ nm and for $t < 18$ nm approximately for NGO.

For films on STO and on LAO, we have also plotted (crosses) the value of T_C as deduced from the strain states (see Table I) within the Millis model:

$$T_C(\epsilon) = T_C(\epsilon=0) \left(1 - \alpha \epsilon_B - \frac{1}{2} \Delta \epsilon^{*2} \right), \quad (1)$$

where $\alpha = 1/T_C dT_C/d\epsilon_B$ and $\Delta = 1/T_C d^2T_C/d\epsilon^{*2}$. For these two magnitudes, we take values from Ref. 23, i.e., $\alpha = 10$ and $\Delta \approx 1000$.

In the case of films on LAO, this model predicts a reduction of T_C , as observed (although the computed T_C value differs from the experimental one by about 20 K). However, for films on STO, the theoretical T_C is almost constant, as expected for films with similar strain states, which is in strong discrepancy with experimental data. Thus we should conclude that the relative agreement between the model and the experiment in the case of LCMO/LAO is probably fortuitous. On the contrary, the experimental observation of a decrease of T_C for unrelaxed films on NGO and STO provides conclusive indications that strain is not the main factor responsible for the disruption of the magnetoelectronic properties of the films when t is reduced.

D. Magnetoresistance

The magnetoresistance (MR) of the films was measured at 10 K as a function of the magnetic field; see Fig. 6. We first notice the absence of any low-field MR like the one which is observed in ceramic samples³⁰ or in films with large grain-boundaries densities.³¹ This is a clear evidence that the films have a low density of structural defects. In agreement with this observation, the thicker films show a small MR value at 90 kOe (typically less than 5%) which indicates that they

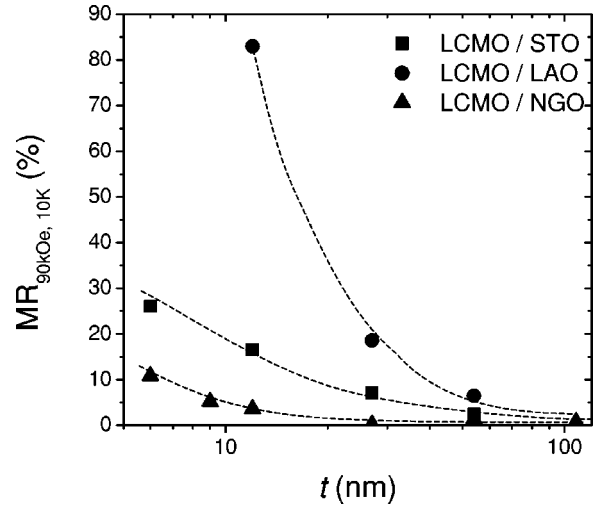


FIG. 7. Magnetoresistance measured at 10 K and 90 kOe as a function of film thickness for the LCMO/STO, LCMO/NGO, and LCMO/LAO series.

contain a small amount of regions with noncollinear magnetic order. When t decreases, the MR increases systematically and more prominently for films on STO and LAO. This is represented in Fig. 7 where we plot the thickness dependence of the MR at 90 kOe and 10 K for all films.

This result suggests that spin-disordered regions are located at interfaces and that their density and/or disorder is more important in the case of LAO and of STO. In addition to this MR increase for low t values, the field dependence becomes hysteretic for films on STO and LAO. This is particularly striking for the 12-nm film on LAO and this MR dependence resembles that of charge-ordered samples like $\text{Pr}_{1-x}\text{Ca}_x\text{MnO}_3$.³² It thus suggests that charge-ordered regions may be present at least in this film and the picture of an inhomogeneous magnetoelectronic texture emerges. The existence of this type of regions possibly extending deep into the film, together with that of metallic zones, is compatible with the hysteresis observed in the magnetoresistance curves and with the conclusion of the resistivity data analysis.

E. Nuclear magnetic resonance

We have carried out the NMR experiment on films on NGO and on STO with $6 \leq t \leq 108$ nm. In Fig. 8 we present the NMR spectra for two 27-nm-thick films, which display features typical for both series of samples. The main resonance occurs around 375 MHz and can be attributed to $\text{Mn}^{3+/4+}$ states in metallic regions.³³ The frequency corresponding to the maximum signal intensity is slightly different for these two films, i.e., 374.5 MHz for LCMO/STO and 378.0 MHz for LCMO/NGO. This NMR line is the dominant response for both films, in agreement with the resistivity data which reveal the metallic character of electric conductance. In addition to this main line, another (low intensity) resonance is detected around 310–320 MHz. A NMR line of similar frequency has been observed in ferromagnetic manganites with semiconducting properties and attributed to Mn^{4+} states.³³ Our observation of the low intensity signal

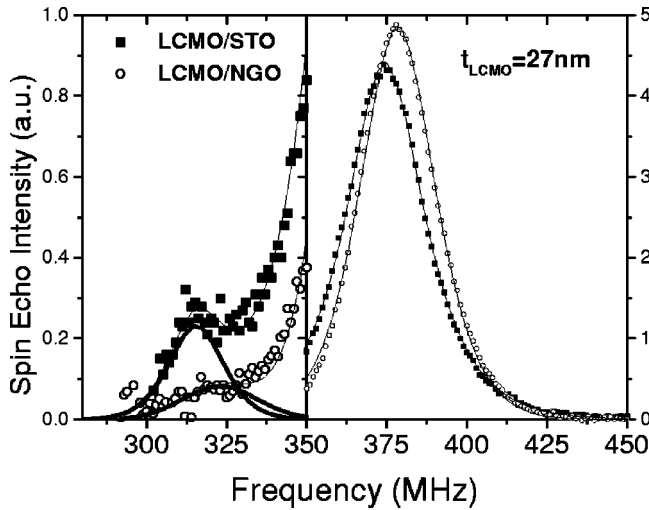


FIG. 8. ^{55}Mn NMR spectra recorded at 4.2 K for two LCMO films of 27 nm.

around 310–320 MHz may thus evidence the presence of regions with low mobility charges. We conclude from this rough analysis that our LCMO films are indeed electronically inhomogeneous, even when grown on a very low mismatch substrate like NGO. For all the films grown on STO and NGO both signals have a high NMR enhancement factor, on the order of 1000, typical of ferromagnetic interactions. We thus conclude that the 370–380-MHz line reflects the presence of a ferromagnetic-metallic (FM) phase while the 320-MHz line is attributed to the existence of ferromagnetic-poorly conducting or ferromagnetic-insulating regions (FI).

We have also studied how the amplitude of these NMR lines changes when thickness increases. It is found that the intensity of the resonance assigned to $\text{Mn}^{3+/4+}$ shows a linear dependence for both series, within experimental error, while the amplitude of the line due to the presence of Mn^{4+} states shows a different behavior depending on the substrate [Fig. 9(a)]. For LCMO/STO, the intensity of the Mn^{4+} line (I^{4+}) increases rapidly for small thickness values and saturates when t reaches 40 nm approximately while for LCMO/NGO, I^{4+} shows a smoother increase with t . These results suggest that in the case of films on STO, the regions with low-mobility charges are mostly located near the interface with the substrate and that for the LCMO/NGO series, these regions are present at any depth in the manganite.

In Figs. 9(b) and (c) we plot the total intensity of the signal detected in NMR as a function of t . As expected for an intensity that has been normalized to the sample area, a linear dependence is found for both series of samples but the extrapolation of the data show zero intensity for a finite thickness which corresponds to regions of the samples that do not respond in NMR. Since all the signal detected in the NMR spectra can be ascribed to nuclei with ferromagnetic interactions, this experimental observation suggests that non-ferromagnetic regions are also present in the films. The effective thickness at which the total NMR intensity becomes zero is 5.3 ± 0.9 nm for LCMO/STO and 6.5 ± 0.2 nm for LCMO/NGO. This thickness is very similar to the dead layer

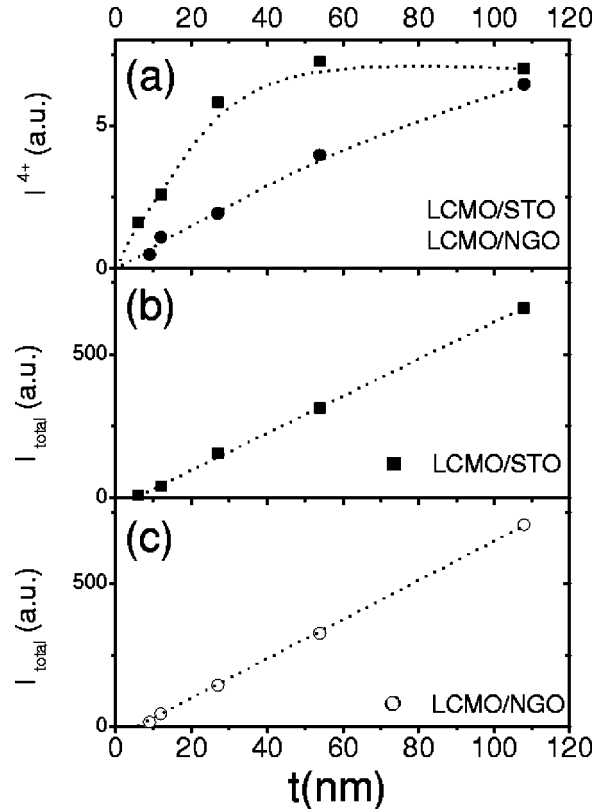


FIG. 9. Thickness dependence of the intensity of the Mn^{4+} line (a) and of the total intensity seen in NMR, (b) and (c), normalized to sample area.

thickness calculated from conductance curves which may be an indication that this third phase is nonferromagnetic and insulating (NFI).

We now analyze the FM phase in more detail and plot the resonance frequency of the $\text{Mn}^{3+/4+}$ line ($f^{3+/4+}$) as a function of thickness; see Figs. 10(a) and (b). For both series, $f^{3+/4+}$ increases with t . It has been suggested by Leung and Morrish³⁴ that, in mixed-valence manganite systems, the resonance frequency of the $\text{Mn}^{3+/4+}$ line ($f^{3+/4+}$) is proportional to the average spin of the Mn ions, i.e., $f^{3+/4+}$ decreases with increasing the doping level x . We therefore interpret the dependence of $f^{3+/4+}$ with t as reflecting modifications in the density of itinerant charge carriers in the

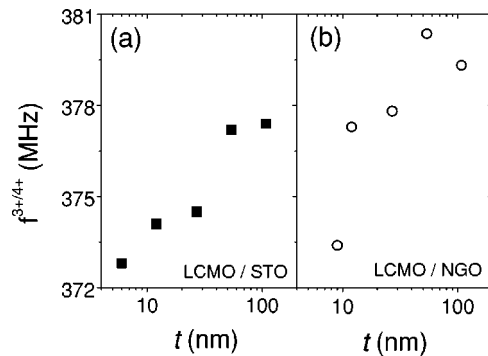


FIG. 10. Thickness dependence of the frequency of the $\text{Mn}^{3+/4+}$ line for films on STO (a) and on NGO (b).

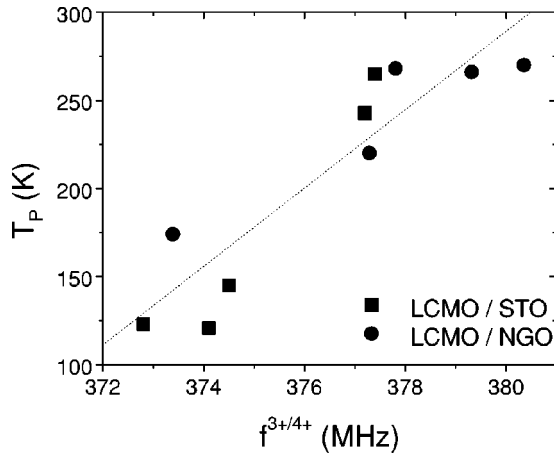


FIG. 11. Relation between $f^{3+/4+}$ and the metal-to-insulator temperature of the films on STO (squares) and on NGO (circles).

FM phase. Since, in the $\text{La}_{1-x}\text{Ca}_x\text{MnO}_3$ phase diagram, deviations from the $x=1/3$ optimal doping value lead to a decrease of the Curie temperature,³⁵ we can expect this change in the effective density of carriers to affect the T_C of our films. We display the relation between T_C and $f^{3+/4+}$ in Fig. 11. Within experimental error, all data fall roughly on a straight line, indicating that the alteration of the density of carriers in the FM phase is certainly one of the factors responsible for the reduction of T_C when t decreases.

IV. DISCUSSION

The results of magnetotransport and NMR measurements all indicate an inhomogeneous magnetoelectronic structure of our LCMO films. In this section we will first discuss the effect of the presence of nonferromagnetic-metallic phases on the metal-to-insulator transition and afterwards analyze the possible reasons for the nucleation of these phases.

Since the values of T_P of our films show a significant thickness dependence even though the cell parameters stay virtually constant, the first important conclusion of this study is that strain does not determine the value of the Curie temperature in manganite films. The observation that T_P for a given thickness, say $t=12$ nm, is different depending on the substrate used (121 K for STO, 220 K for NGO, and 95 K for LAO) also indicates that simple dimensional effects (see for instance Zhang and Willis³⁶) are not mainly responsible for the observed variation. We argue here that the observed decrease of T_P is closely linked to the presence of non-FM regions in the films which reduces the effective ferromagnetic coupling in the metallic phase. The correlation between T_P and $f^{3+/4+}$, illustrated by Fig. 11, is a clear indication that a modification in the density of itinerant carriers in the FM regions is to a great extent the driving factor for the decrease of T_P observed for thinner films. This can be due either to a change in the stoichiometry with thickness (for instance low oxygen content) or to localization of some e_g electrons. The observation of two insulating phases in these films support the picture of electron trapping in insulating regions.

Among other possible causes that lead to a decrease of T_C

in manganites, bond length and angle disorder have shown to have a significant impact.³⁷ Indeed, in metallic $\text{La}_{1-x}\text{Ca}_x\text{MnO}_3$ Mn-O distances take a single value while in insulating orthorhombic manganites, several distinguishable Mn-O bond lengths can exist due to Jahn-Teller distortion at Mn^{3+} sites.³⁸ Since in our films, regions with localized charges coexist with metallic zones, we can expect the MnO_6 octahedra located in the FM phase near boundaries with the insulating regions to be distorted. Thus a substantial dispersion of the Mn-O distances and Mn-O-Mn angles is likely to exist to some extent in the FM phase. This should promote a shrinking of the bandwidth and thus a further reduction of the Curie temperature³⁸ in the films for which the proportion of insulating regions is large, i.e., in thinner films. This effect can be taken as a second factor responsible for the decrease of T_P when t diminishes.

We now discuss the possible origin of phase separation in these films. Recently it has been predicted that a small amount of disorder in the magnetic interactions (double exchange and superexchange) in a ferromagnetic homogeneous system can lead to the nucleation of antiferromagnetic regions.³⁹ This mechanism can be at the origin of the inhomogeneity of our films. Since the parasitic phases are more prominently located at interfaces, substrate-induced disorder could be responsible for the observed phase separation. This disorder can arise from the coexistence of different atomic terminations at the surface of the substrate at the beginning of the growth. Indeed, it has been reported that commercial STO substrates generally present two types of terminations, namely SrO or TiO_2 .⁴⁰ In this case, it is expected that the manganite grows with (La, Ca)O planes on top of TiO_2 terminations and MnO_2 planes on SrO terminations. The existence of these two possible environments for the Mn ions at the interface could promote electron localization in highly distorted sites (MnO_2/SrO type) as well as the coexistence of a variety of Mn-O distances and Mn-O-Mn angles. This would certainly induce a substantial disorder in the values of the magnetic interactions constants and, consequently, within the model of Moreo *et al.*,³⁹ to the nucleation of parasite phases. The difference in the thickness dependence of I^{4+} between the LCMO/STO and LCMO/NGO series can arise from different growth mechanisms in the first stages of the LCMO deposition. The factors controlling this precise stage are not well known but substrate roughness and strain certainly play an important part.

To validate this hypothesis systematic studies on films grown on substrates with a single atomic termination⁴¹⁻⁴⁴ are needed. Indeed, it has been reported recently that the use of single-terminated substrates as opposed to as-received ones could increase the T_P of LCMO films by some 20 K.⁴⁵ Similar finding has been reported for $\text{YBa}_2\text{Cu}_3\text{O}_x$ films.⁴⁶ This provides evidence that this type of substrate-induced disorder plays an important role in determining the magnetoelectronic properties of oxides thin films. Its minimization, and more globally the control at atomic scale⁴⁷ of interfaces in heterostructures of manganites, appears essential to obtain substantial magnetoresistive response at room temperature in manganite-based devices.

V. CONCLUSION

We have performed magnetotransport and ^{55}Mn NMR measurements on LCMO films of thicknesses ranging from 2.4 to 108 nm grown on STO, NGO, and LAO substrates. It is found that the resistivity and the low-temperature MR increase strongly when thickness is reduced, which is accompanied by a shift of the metal-to-insulator transition towards low temperatures. Since our LCMO/STO and LCMO/NGO films have similar cell parameters within a same series, we discard strain and dimensional effects as the cause of the observed thickness dependence of T_p . The analysis of the NMR spectra performed on these two series shows that the films have an inhomogeneous magnetoelectronic texture with ferromagnetic-insulating and nonferromagnetic-insulating regions coexisting within a ferromagnetic-metallic phase. These parasitic phases are mainly located at interfaces in the case of STO substrates but more homogeneously distributed in the case of NGO. More importantly, we have identified a clear correlation between the resonant frequency of the main NMR line and the variation of the Curie temperature with thickness, which we interpret as a strong evidence of carrier density modifications. We argue that the presence of nonferromagnetic-metallic phases and the subsequent localization of e_g electrons are at the origin of the observed lowering of T_p . The presence of these insulating regions can also induce a shrinking of the bandwidth due to disorder in Mn-O distances and Mn-O-Mn angles, causing an additional decrease of T_p .

The origin of this phase separation appears to be related to

the nature of the substrate. However, we have shown that there is not a simple correlation with structural mismatch between LCMO and substrate. We thus suggest that the differences observed in the behavior of the LCMO/STO and LCMO/NGO series arise from different microstructural characteristics of the films, probably related to differences in growth mechanisms and atomic terminations of the uppermost atomic layers of the substrates. Control and engineering at atomic scale are thus a requisite to obtain electronically sharp interfaces and to avoid spurious electronic segregation. Alternatively this study shows that the electronic phase segregation is not simply an intrinsic property of these perovskites (at optimal doping) but can result from surface effects. Disorder in the magnetic interactions, and especially in the double exchange integral, could be generated by the coexistence of various environments for the Mn ions just at the interface, due to the use of non single-terminated substrates.

ACKNOWLEDGMENTS

Financial support by the EEC OXSEN, the CICYT MAT2000-1290-C03-03 and MAT1999-0984-C03-01 (Spain) project and the Ford Motor Company (Poland) are acknowledged. This work has also been supported in part by the NATO Collaborative Linkage Grant PST.CLG.978518. The authors are very grateful to M.-J. Casanove for HREM analysis. Many thanks must be addressed to A. Barthélémy, F. Pailloux, A. Anane, L. Ranno, F. Sandiumenge, and M. Bowen for helpful discussions.

*Electronic address: manuel.bibes@thalesgroup.com

¹J.M.D. Coey, M. Viret, and S. von Molnar, *Adv. Phys.* **48**, 167 (1999).

²E. Dagotto, T. Hotta, and A. Moreo, *Phys. Rep.* **344**, 1 (2001).

³M. Viret, M. Drouet, J. Nassar, J.-P. Contour, C. Fermon, and A. Fert, *Europhys. Lett.* **39**, 545 (1997).

⁴Y. Lu, W. Li, G.Q. Gong, G. Xiao, A. Gupta, P. Lecoeur, J.Z. Sun, Y.Y. Wang, and V.P. Dravid, *Phys. Rev. B* **54**, R8357 (1996).

⁵M.H. Jo, N.D. Mathur, N.K. Todd, and M.G. Blamire, *Phys. Rev. B* **61**, R14 905 (2000).

⁶K.R. Nikolaev, A. Yu Dobin, I.N. Krivorotov, W.K. Cooley, A. Bhattacharya, A.L. Kobrinski, L.I. Glazman, R.M. Wentzovitch, E.D. Dahlberg, and A.M. Goldman, *Phys. Rev. Lett.* **85**, 3728 (2000).

⁷Z.W. Dong, R. Ramesh, T. Venkatesan, M. Johnson, Z.Y. Chen, S.P. Pai, V. Talyansky, R.P. Sharma, R. Shreekala, C.J. Lobb, and R.L. Greene, *Appl. Phys. Lett.* **71**, 1718 (1997).

⁸J.-H. Park, E. Vescovo, H.J. Kim, C. Kwon, R. Ramesh, and T. Venkatesan, *Phys. Rev. Lett.* **81**, 1953 (1998).

⁹M. Calderón, L. Brey, and F. Guinea, *Phys. Rev. B* **60**, 6698 (1999).

¹⁰F. Ott, M. Viret, R. Borges, R. Lyonnet, E. Jacquet, C. Fermon, and J.-P. Contour, *J. Magn. Magn. Mater.* **211**, 200 (2000).

¹¹F. Pailloux *et al.* (unpublished).

¹²H.S. Wang, E. Wertz, Y.F. Hu, Q. Li, and D.G. Schlom, *J. Appl. Phys.* **87**, 7409 (2000).

¹³R.A. Rao, D. Lavric, T.K. Nath, C.B. Eom, L. Wu, and F. Tsui,

Appl. Phys. Lett. **73**, 3294 (1998).

¹⁴R.B. Peraus, G.M. Gross, F.S. Razavi, and H.-U. Habermeier, *J. Magn. Magn. Mater.* **211**, 41 (2000).

¹⁵M. Bibes, Ll. Balcells, S. Valencia, B. Martínez, M.-J. Casanove, J.-C. Ousset, and J. Fontcuberta, *Appl. Surf. Sci.* **188**, 202 (2002).

¹⁶J.Z. Sun, D.W. Abraham, R.A. Rao, and C. Eom, *Appl. Phys. Lett.* **74**, 3017 (1999).

¹⁷M. Ziese, *Phys. Rev. B* **60**, R738 (1999).

¹⁸R.P. Borges, W. Guichard, J.G. Lunney, J.M.D. Coey, and F. Ott, *J. Appl. Phys.* **89**, 3868 (2001).

¹⁹J.Z. Sun, *Philos. Trans. R. Soc. London, Ser. A* **356**, 1693 (1998).

²⁰H.W. Zandbergen, S. Fresien, T. Nojima, and J. Aarts, *Phys. Rev. B* **60**, 10 259 (1999).

²¹A. Biswas, M. Rajeswari, R.C. Srivastava, Y.H. Li, T. Venkatesan, R.L. Greene, and A.J. Millis, *Phys. Rev. B* **61**, 9665 (2000).

²²M. Izumi, Y. Konishi, T. Nishihara, S. Hayashi, M. Shinohara, M. Kawasaki, and Y. Tokura, *Appl. Phys. Lett.* **73**, 2497 (1998).

²³A.J. Millis, T. Darling, and A. Migliori, *J. Appl. Phys.* **83**, 1588 (1998).

²⁴J. Zhang, H. Tanaka, T. Kanki, J.-H. Choi, and T. Kawai, *Phys. Rev. B* **64**, 184404 (2001).

²⁵T. Kanki, H. Tanaka, and T. Kawai, *Phys. Rev. B* **64**, 224418 (2001).

²⁶M. Bibes, Ll. Balcells, S. Valencia, J. Fontcuberta, M. Wojcik, E. Jedryka, and S. Nadolski, *Phys. Rev. Lett.* **87**, 067210 (2001).

²⁷M. Bibes, Ll. Balcells, S. Valencia, S. Sena, B. Martínez, J. Font-

- cuberta, S. Nadolski, M. Wojcik, and E. Jedryka, *J. Appl. Phys.* **89**, 6686 (2001).
- ²⁸S. Bueble, K. Knorr, E. Brecht, and W. Schmahl, *Surf. Sci.* **400**, 345 (1998).
- ²⁹M. Wojcik *et al.* (unpublished).
- ³⁰L. Balcells, B. Martínez, and J. Fontcuberta, *Phys. Rev. B* **58**, R14 697 (1998).
- ³¹J. Gu, S. Ogale, M. Rajeswari, T. Venkatesan, R. Ramesh, V. Radmilovic, U. Dahmen, G. Thomas, and T. Noh, *Appl. Phys. Lett.* **72**, 1113 (1998).
- ³²W. Prellier, Ch. Simon, B. Mercey, M. Hervieu, A.M. Haghiri-Gosnet, D. Saurel, Ph. Lecoœur, and B. Raveau, *J. Appl. Phys.* **89**, 6612 (2001).
- ³³G. Matsumoto, *J. Phys. Soc. Jpn.* **29**, 615 (1970).
- ³⁴L.K. Leung and A.H. Morrish, *Phys. Rev. B* **15**, 2485 (1972).
- ³⁵P. Schiffer, A.P. Ramirez, W. Bao, and S.-W. Cheong, *Phys. Rev. Lett.* **75**, 3336 (1995).
- ³⁶R. Zhang and R. Willis, *Phys. Rev. Lett.* **86**, 2665 (2001).
- ³⁷L.M. Rodríguez-Martínez and J.P. Attfield, *Phys. Rev. B* **54**, R15 622 (1996).
- ³⁸P. Radaelli, M. Marezio, H. Hwang, S.-W. Cheong, and B. Batlogg, *Phys. Rev. B* **54**, 8992 (1996).
- ³⁹A. Moreo *et al.*, *Phys. Rev. Lett.* **84**, 5568 (2000).
- ⁴⁰M. Kawasaki, K. Takahashi, T. Maeda, R. Tsuchiya, M. Shinohara, O. Ishiyama, T. Yonezawa, M. Yoshimoto, and H. Koinuma, *Science* **266**, 1540 (1994).
- ⁴¹G. Koster, B. Kropman, G. Rijnders, D. Blank, and H. Rogalla, *Appl. Phys. Lett.* **73**, 2920 (1998).
- ⁴²K. Iwahori, S. Watanabe, M. Kawai, K. Mizuno, K. Sasaki, and M. Yoshimoto, *J. Appl. Phys.* **88**, 7099 (2000).
- ⁴³T. Ohnishi, K. Takahashi, M. Nakamura, M. Kawasaki, M. Yoshimoto, and H. Koinuma, *Appl. Phys. Lett.* **74**, 2531 (1999).
- ⁴⁴V. Leca, G. Rijnders, D. Blank, and H. Rogalla, presentation of the E-MRS meeting, Strasbourg, France, 2001.
- ⁴⁵P. Padhan, N. Pandey, S. Srivastava, R. Rakshit, V. Kulkarni, and R. Budhani, *Solid State Commun.* **117**, 27 (2001).
- ⁴⁶T. Nakamura, H. Inada, and M. Iiyama, *Appl. Surf. Sci.* **130-132**, 576 (1998).
- ⁴⁷J. Choi, C. Eom, G. Rijnders, H. Rogalla, and D. Blank, *Appl. Phys. Lett.* **79**, 1447 (2001).